

# Implantation of a holographic structure and waveguide periodic structures formed by silver nanoparticles into AgCl–Ag film and quartz glass

*K.S.Beloshenko, L.A.Ageev, V.K.Miloslavsky*

V.Karazin Kharkiv National University, Physical Optics Chair,  
4 Svobody Sq., 61077 Kharkiv, Ukraine

*Received February 11, 2010*

A holographic grating (HG) with period  $\Lambda = 2 \mu\text{m}$  has been formed in an AgCl–Ag film on a glass substrate using two symmetric laser beams ( $\lambda = 532 \text{ nm}$ ). A nonlinear self-diffraction effect takes place at the HG formation. The light-generated structure has been implanted into quartz by irradiating with a  $\text{CO}_2$  laser beam.

В фоточувствительной пленке AgCl–Ag на стеклянной подложке двумя симметричными лазерными пучками ( $\lambda = 532 \text{ нм}$ ) записана голографическая решетка (ГР) с периодом  $\Lambda = 2 \text{ мкм}$ . При формировании ГР имеет место нелинейный эффект самодифракции. Сформированная светом структура имплантирована в кварц путем облучения образца пучком  $\text{CO}_2$  лазера.

## 1. Introduction

The implantation of metal nanoparticles into dielectrics draws attention in connection with development of nanosize object physics, nonlinear optics, and optoelectronics [1, 2]. The silver chloride films coated with a thin island silver layer (the AgCl–Ag films) are known to show a photosensitivity to the visual spectral range radiation and to provide periodic structures (PS) consisting of silver particles due to waveguide and nonlinear properties [3–5]. The PS implanted with light into AgCl under action of one S- or P-polarized monochromatic beam on an AgCl–Ag film. The PS are known to arise also under action of two beams that form a holographic grating (HG) in the film [6]. In [6], the S-polarized laser beams were used and the PS development was considered as an adverse factor resulting in reduced diffraction efficiency of the HG. Note that the noise PS under action of two crossing laser beams were observed to arise in

photorefractive crystals, too [7]. It is the space orientation of the linear polarization direction  $\mathbf{E}$  of the active beams that is of importance for the PS development in AgCl–Ag. In this work, the HG and PS recording at two symmetrical beams with  $\mathbf{E}$  oriented at  $45^\circ$  to the plane of incidence onto the film has been realized for the first time. It has been found that the linear self-diffraction effect [5, 8] appearing at the HG recording is of a great importance in the PS development.

To prepare the films, various dielectric substrates can be used, for example, the optical quartz glass (OQG). At present, several methods are known to implant the colloidal metallic particles into silicate glasses [1, 9]. However, some of those are unsuitable to implant the particles into OQG. The ion-exchange chemical reactions are inapplicable as the implantation method due to absence of impurities in the OQG that are usual in silicate glasses. The thermally stimulated implantation is another example.

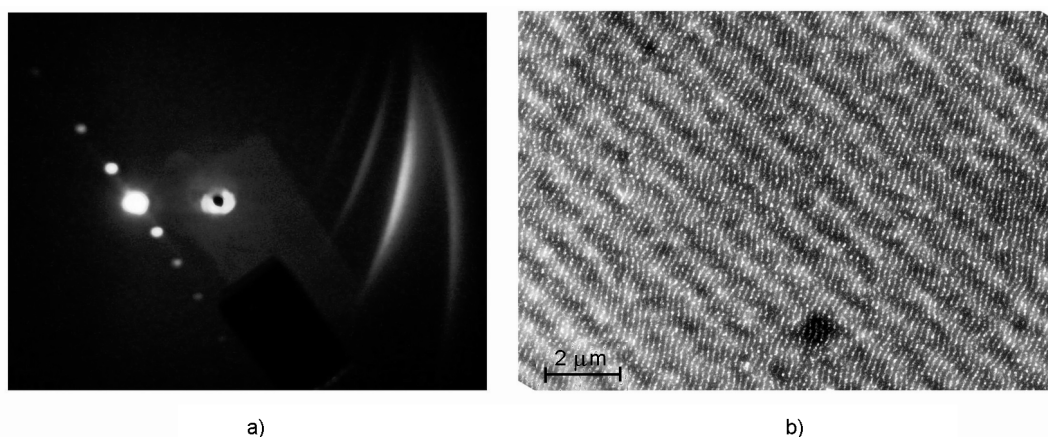


Fig. 1. Diffraction pattern (a) and micrograph (b) of structure forming the diffraction pattern (a). The structure (b) scale is defined by the broad parallel bends of the holographic grating with period  $2 \mu\text{m}$ .

There are data on the OQG coloration with colloidal copper when during the high-temperature annealing of the glass in a furnace including copper-containing parts [10]. At the same time, there is only scarce information in literature on the possibility of colloidal silver thermostimulated implantation into OQG [9]. Recently, the isotropic colloid was implanted into the near-surface layer of OQG by heating the island Ag film at the OQG surface using a  $\text{CO}_2$  laser beam [11, 12]. Further studies of that method have shown that it is possible to implant into OQG not only isotropic colloid but also ordered structures consisting of silver particles [13]. In this work, the HG and PS formed at the OQG surface by thermostimulated implantation of the HG and PS into the AgCl–Ag film followed by its fixation have been implanted into OQG using the same implantation technique.

## 2. Experimental

About 2 mm thick plates of OQG (KU grade) and optical glass (K-8 grade) were used in our experiments. An AgCl film of about 35 nm thickness was thermally sputtered onto the plate in vacuum and then an about 10 nm thick island Ag film was deposited thereon. The AgCl–Ag film is directly photosensitive to irradiation within the whole visible spectral range. The standard double-beam interference scheme of polarized laser beams ( $\lambda_0 = 532 \text{ nm}$ ,  $P = 25 \text{ mW}$ ) was used to record the HG. The interference bands were oriented perpendicular to the convergence plane of two beams. Both the light beams were of the same intensity and converged in a horizontal plane of incidence onto the film. The polarization directions  $\mathbf{E}$

of the beams make angle of  $45^\circ$  with the incidence plane. The light-induced transformations at the HG recording should occur in the film areas corresponding to the interference maxima. A specific feature of the AgCl–Ag films consists in that in the holographic interference maxima, the PS connected with the excitation of waveguide modes are induced and developed, too [3–5], and the PS grooves penetrate partially also the area of holographic minima. As a consequence, a combined structure consisting of HG and PS gratings is formed in the film due to the Ag photostimulated implantation.

The HG and PS were recorded at the exposure time of 30 min that corresponds approximately to the development of the structures till saturation. Due to photoinduced implantation, the most part of silver goes from the AgCl–Ag film surface to the film/substrate interface. After the irradiation was over, the AgCl film was removed by dissolving it in fixer (aqueous hyposulfite solution) followed by the sample washing in water, the excess water was removed from the surface by air blowing. In those conditions, the structure pattern and diffraction properties are retained but the photosensitivity of the sample disappears [4]. To observe the whole diffraction pattern at small incidence angles, a UV beam from a nitrogen laser ( $\lambda = 337 \text{ nm}$ ) was used. To improve the reflection factor and the diffraction efficiency, the sample was coated in vacuum with a thin (about 50 nm) aluminum mirror. The Al layer provides also the conductivity of the sample surface and makes it possible to study the structure using a SEM (JSM-80070,  $U = 20 \text{ kV}$ , spatial resolution 3 nm). The thermostimulated

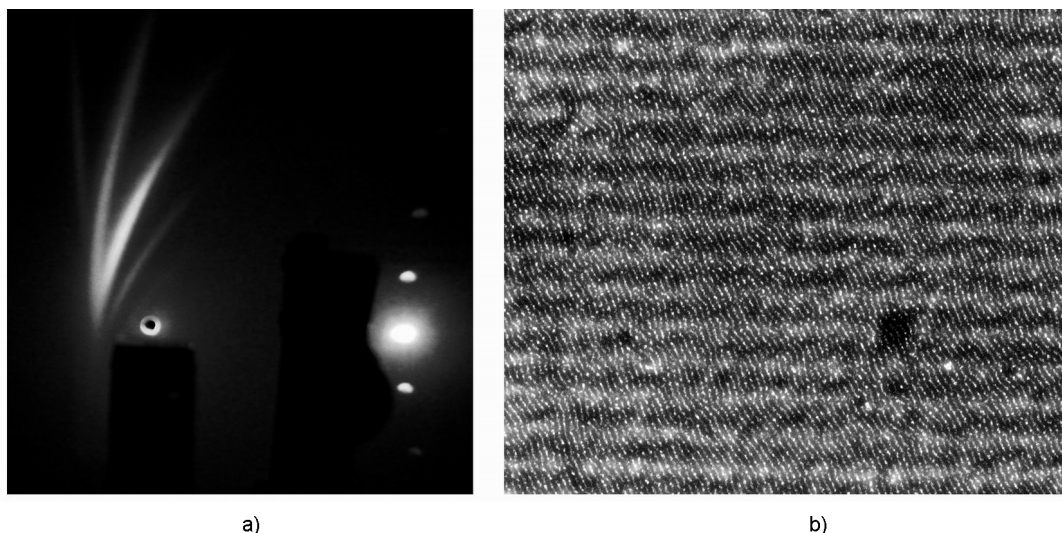


Fig. 2. The figure differs from Fig. 1 in the sample orientation. The structure micrograph is orientes so that the spatial position of the structure periodic elements corresponds to the diffraction pattern.

implantation of the interference structures into OQG was carried out using a CO<sub>2</sub> laser beam ( $\lambda = 10.6 \mu\text{m}$ ,  $P = 20 \text{ W}$ ), the exposure time being about 1 min. The retained periodicity of the implanted structures (HG and PS) is evidenced by retained diffraction properties thereof.

### 3. Results and discussion

Fig. 1a presents the diffraction pattern from a fixed and aluminum-coated sample. The diffraction from HG is seen in the left-hand figure part as symmetrical light spots located along a line. The brightest spot is formed by the specular beam. In the right part, there are four discrete arc-shaped bands that correspond to diffraction from the PS formed in the film. The sample is placed on a horizontal goniometer, and in the position shown in the photo, the PS periods  $d$  were measured. When measuring, the incidence angle  $\varphi$  was increased so that the diffraction band coincided with the hole in the screen, that corresponds to the autocollimation condition (the diffraction beam is directed opposite to the incident one and  $\varphi = -\varphi_a$ ,  $\varphi_a$  being the autocollimation angle). At  $\varphi$  close to  $\varphi_a$ , the 5<sup>th</sup> band becomes visible in the diffraction pattern from PS. For PS, all the diffraction bands correspond to the "-1" order diffraction and the periods are calculated from the measured  $\varphi_a$  angles as  $d = \lambda(2\sin\varphi_a)^{-1}$ . However, to measure the PS period at high accuracy, a small section of an arc-shaped band with maximum intensity is to be used.

Due to differences in curvature, slopes, and spatial positions of the bands with respect to the horizontal line of angle measurement, the measurement errors for different bands differ considerably. The highest error is found for weak side bands. The measurement results for the bands 1 through 5 (from left to right) are as follows:

$$\begin{aligned} d_1 &= 470 \pm 10\text{nm}; & d_2 &= 421 \pm 3\text{nm}; & (1) \\ d_3 &= 373 \pm 1\text{nm}; & d_4 &= 331 \pm 1\text{nm}; \\ d_5 &= 301 \pm 10\text{nm}. \end{aligned}$$

To present the diffraction pattern more precisely, Fig. 2a shows the diffraction observed after the sample was rotated about the normal into the position providing the vertical arrangement of the diffraction spots from HG. When comparing Fig. 1a and Fig. 2a, it is to note that in the first case, the incidence angle was adjusted by rotating the goniometer counterclockwise while in the second one, clockwise. That is why the diffraction bands from PS in the photos diverge oppositely (down and up) and are in different positions (right, left). Moreover, the angle of incidence in the 2<sup>nd</sup> case exceeds about twice that in the 1<sup>st</sup> one. The increase of the incidence angle results in increased curvature of the line where the HG diffraction reflections are arranged (round spots in the photo, positioned right). If the former band numbering is retained (but now from right to left), the diffraction band 1 from PS is weak but the band 5 is seen clearly. Moreover, the tangency point of bright bands 3 and 4 is seen well. This point

is positioned at the horizontal and makes it possible to measure the autocollimation angle corresponding thereto. The period  $d_0$  determined from that angle is 350 nm.

The HG period  $\Lambda$  was measured, too. To that end, the sample was rotated about the normal to it so that the line where the diffraction spots of different orders are arranged is horizontal and passed the hole in the screen. The measurements provided the value  $\Lambda = 2 \pm 0.005 \mu\text{m}$ . That value should coincide with the calculated HG period:

$$\Lambda = \lambda_0 / 2 \sin(\alpha/2). \quad (2)$$

From the measured  $\Lambda$ , the incidence angles  $\varphi$  for both beams are determined:  $\varphi = \alpha/2 = 7.6^\circ$ .

In Fig. 1b and 2b, the SEM images of the sample structure are shown. The images are oriented so that the diffraction patterns are in accordance with the structures. The broad alternating dark and bright bands present the HG grooves and their period ( $\Lambda = 2 \mu\text{m}$ ) points the image scale. A much thinner structure corresponds to the PS. The spatial scatter in the mutual orientation of the PS grooves as well as the scatter thereof with respect to the strictly fixed direction of the HG grooves. It is seen also that the PS are concentrated mainly in the bright HG bands that correspond to the interference maxima at the HG recording. However, in many cases, the PS grooves penetrate also the dark HG bands (the holographic interference minima). Those features evidence a gradual HG deterioration during the PS development. The HG deterioration should be manifested most strongly if both HG and PS have similar periods [6]. In this experiment, the HG to PS period ratio is high ( $\Lambda/d = 5$ ). That is why the HG are not broken completely. The HG diffraction efficiency of the HG remains high also at exposures corresponding to the saturation in the HG development.

*Interrelation between HG and PS.* The existence of an interrelation between the HG and PS is the most interesting result from the viewpoint of the structure development. That interrelation makes it possible to explain why the PS with different periods indicated in (1) arise. The AgCl–Ag film is a nonlinear medium and the HG are recorded therein according to the laws of nonlinear self-diffraction effect. The components  $k_x^\delta$  of the wave vectors of the diffracted beams on the film plane are related to the components  $k_x$  of the acting beams [5] as

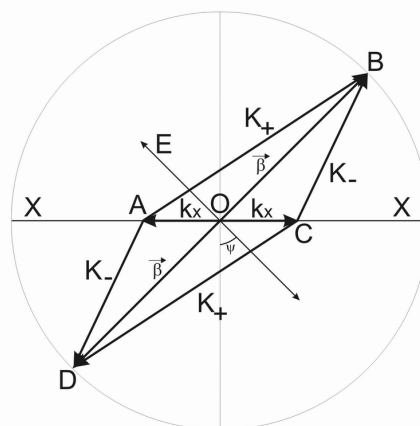


Fig. 3. Polar diagram illustrating the formation of periodic structures under action of two incident beams. O is the incidence point of the beams;  $k_x$ , the projections of the incident beam wave vectors onto the film plane; XX, the incidence plane trace on the film;  $\mathbf{E}$ , the direction of the beam linear polarization;  $\beta$ , the predominant directions and values of the wave vectors of the scattered waveguide modes;  $\mathbf{K}_{+,-}$  – the vectors of the PS formed.

$$k_x^\delta = (2m \pm 1)k, \quad (3)$$

where  $m = \pm 1, \pm 2, \dots$  are the diffraction orders; the signs + and – refer to the beams (1) and (2), respectively. It is seen from (3) that at different combinations of  $m$ , the components  $k_x^\delta$  have values

$$k_x^\delta = pk; \quad p = \pm 1, \pm 3, \pm 5, \dots \quad (4)$$

The PS are nucleated due to interference of the incident beam and waveguide modes that appear in the film due to the Rayleigh scattering of the incident beam. The development of PS occurs according to the positive feedback mechanism: the PS nucleation results in an amplification of the mode, thus favoring the further PS growth. At a small thickness of the AgCl film (about 35 nm), only the  $\text{TE}_0$  type limiting mode is excited therein with the effective refractive index  $n_c$  equal to that of the substrate (at  $\lambda_0 = 532 \text{ nm}$ ,  $n_c = 1.52$  for K-8 and  $n_c = 1.46$  for OQG) [4, 13]. The predominant scattering direction of the mode is that perpendicular to the polarization direction  $\mathbf{E}$  of the inducing light wave incident the film. Let the vector  $\mathbf{K}$  be that of PS ( $K = 2\pi/d$ );  $\beta$ , the wave vector of the mode (the mode propagation constant  $\beta = (2\pi/\lambda_0)n_c$ ) and  $k_x$ , the component of the incident wave vector at the film

surface ( $k_x = (2\pi/\lambda_0)\sin\varphi$ ). The PS development is defined by the formula [4, 13]

$$\mathbf{K} = \boldsymbol{\beta} - \mathbf{k}_x. \quad (5)$$

The sense of condition (5) is disclosed by the vector diagram shown in Fig. 3. The diagram is referred to the film plane and constructed in the orientation according to the film irradiation conditions (the incidence plane is horizontal). The point O is the incidence point of the beams. The XX line is that of the incidence plane intersection with the film. The direction of the beam linear polarization is shown by the line **E**. The angle  $\psi = 45^\circ$ . The vectors  $\boldsymbol{\beta}$  show the predominant directions and values of the propagation constants for the modes scattered in opposite directions. The components  $\mathbf{k}_x$  correspond to two incident beams. When only one beam is acting (e.g., that with the right-hand component  $\mathbf{k}_x$ ), the modules of PS vectors are determined from  $\Delta OBC$  and  $\Delta ODC$ :

$$K_{\pm}^2 = \beta^2 + k_x^2 \pm 2\boldsymbol{\beta} \cdot \mathbf{k}_x \cdot \cos\psi. \quad (6)$$

The even PS are formed by the second beam ( $\mathbf{k}_x$  to the left,  $\Delta ODA$  and  $\Delta OAB$ ). The simultaneous action of two symmetrical beams amplifies the PS development, since the values of PS vectors  $K_{\pm}$  are pairwise parallel to each other.

The formula (6) explains the development of two PS with the vector values  $\mathbf{K}_{\pm}$ . However, the diffraction pattern shows that PS with other periods are developed in the film. To explain the additional PS, it is to take into account that those are developed due to action not only of two incident beams but also of the diffraction beams arising during the HG development. The diffraction beams from HG have the wave vector components at the film surface equal to uneven  $k_x$  values (formula (4)). In spite of the fact that those beams are proceeding from the film itself, the field thereof stimulates the PS development similar to the field of the incident beams. Due to such a relation between the HG and PS, it is necessary to use in the formulas (5) and (6) the quantity  $pk_x$  instead of  $k_x$ ; without account for the sign,  $p = 1, 3, 5, \dots$ . Then we get from (6) the formula to calculate the periods of all possible PS:

$$(d_{\pm(p)})_i = \frac{\lambda_0}{(n_c^2 + (p \cdot \sin\varphi)^2 \pm 2p \cdot n_c \cdot \sin\varphi \cdot \cos\psi)^{1/2}}, \quad (7)$$

where  $i = 1, 2, 3, 4, 5$  are the numbers of diffraction bands from PS observed in experiment. The calculations using (7) for experimental values  $\lambda_0 = 532$  nm,  $n_c = 1.52$  (K-8),  $\varphi = 7.6^\circ$ ,  $\psi = 45^\circ$  have given the following results:

$$\begin{aligned} (d_{-(5)})_1 &= 462nm, \dots (d_{-(3)})_2 = 419nm, \\ \dots (d_{-(1)})_3 &= 372nm, \dots (d_{+(1)})_4 = 329nm, \\ \dots (d_{+(3)})_5 &= 292nm. \end{aligned} \quad (8)$$

The periods calculated using (7) agree satisfactorily with those measured ones indicated above (1). Thus, the assumption of the interrelation between the self-diffraction HG and developing PS is valid.

The value  $d_0 = 350$  nm obtained by measurement of the autocollimation position of the intersection point between the bands 3 and 4 (Fig. 2a) corresponds precisely to the period of a PS that would be formed at the normal incidence of the inducing beam with  $\lambda_0 = 532$  nm and vertical linear polarization. As it follows from (5), in this case,  $\mathbf{K} = \boldsymbol{\beta}$  and  $d_0 = \lambda_0/n_c = 350$  nm.

The substantial difference between the diffraction beams from HG and from PS is well seen in Fig. 1a, 2a. The HG being a perfect diffraction grating gives the diffraction beams of the same shape as the measuring laser beam and forming round light spots on the screen. In contrast, the diffraction from PS does not form spots, but arc-shaped bands. That shape of the diffraction beams indicates that the PS as a whole are imperfect diffraction gratings. Those consist of a set of individual microscale gratings that are developed as the modes are scattered on different scattering centers. The modes being excited show an angular scatter with respect to the predominant scattering direction shown in Fig. 3. This results in a scattering of vectors related to different microgratings, thus causing the expansion of the diffraction beam from PS [4].

All the above results are related to the K-8 glass substrate. As to the OQG substrate, the same results are remained, except for the PS periods. They follow also the formula (7) at  $n_c = 1.46$ . As an example, the calculated PS periods corresponding to the coefficient  $p = 1$  in (7) and having the highest diffraction efficiency are as follows:

$$(d_{-(1)})_3 = 388nm; \dots (d_{+(1)})_4 = 342nm. \quad (9)$$

The periods measured for PS on the OQG surface are essentially the same as the calculated ones. The subsequent thermo-stimulated implantation of the structures formed by silver particles into the near-surface OQG layer has been carried out using a CO<sub>2</sub> laser beam (see [13] for details). That is why the implanted structure contains not only the PS with periods (9) but also a regular HG with 2 μm period. The conservation of PS and HG periods after the implantation has been confirmed by diffraction measurements. The fact of implantation itself is confirmed by the structure stability against mechanical and chemical actions, as in [13].

#### 4. Conclusion

In this work, considered has been the photoinduced implantation of colloidal silver nanoparticles into photosensitive AgCl–Ag film on glass substrates under action of two symmetrical laser beams. Due to non-linear light absorption in the film, the Ag particles form the grooves of a holographic grating (HG) that is developed under manifestation of the self-diffraction effect. Considered is the case when the beams acting on the film are linearly polarized at the angle of 45° to the plane of incidence on the film. The linear polarization of the beams results in development, side-by-side HG, of periodical structures (PS) related to excitation of TE<sub>0</sub> type waveguide modes in

the film. The PS have been found to develop not only due to the incident beams but also to the diffraction beams from HG.

#### References

1. U.Kreiber, M.Vollmer, Optical Properties of Metal Clusters, Springer-Verlag, Berlin-Heidelberg (1995).
2. R.A.Geneev, A.I.Ryasnyansky, A.L.Stepanov et al., *Optika i Spekr.*, **95**, 1034 (2003).
3. L.A.Ageev, V.K.Miloslavsky, *Opt. Engin.*, **34**, 960 (1995).
4. L.A.Ageev, V.K.Miloslavsky, H.I.El-Ashkhab, V.B.Blokha, Tutorial Experiments and Demonstrations on Optics: Teaching Aid, Kharkiv Nat. Univ. (2000) [in Russian].
5. V.K.Miloslavsky, Nonlinear Optics: Teaching Aid, Kharkiv Nat. Univ. (2008) [in Russian].
6. L.A.Ageev, V.K.Miloslavsky, V.I.Lymar, *Optika i Spekr.*, **69**, 415 (1990).
7. B.I.Sturman, S.G.Odulov, M.Yu.Goulkov, *Phys.Reports*, **275**, 197 (1996).
8. V.L.Vinetsky, N.V.Kukhtarev, S.G.Odulov, M.S.Soskin, *Usp.Fiz.Nauk*, **129**, 113 (1979).
9. A.L.Stepanov, *Rev.Adv.Mater.Sci.*, **4**, 123 (2003).
10. V.K.Leko, O.V.Mazurin, Properties of Quartz Glass, Nauka, Leningrad (1985) [in Russian].
11. L.A.Ageev, V.K.Miloslavsky, E.D.Makovetsky, *Optika i Spekr.*, **102**, 489 (2007).
12. L.A.Ageev, V.K.Miloslavsky, E.D.Makovetsky et al., *Functional Materials*, **14**, 24 (2007).
13. L.A.Ageev, K.S.Beloshenko, E.D.Makovetsky, V.K.Miloslavsky, *Optika i Spekr.*, **107**, 838 (2009).

## Імплантація голографічної та хвилевідних періодичних структур, утворених нанорозмірними частинками срібла, у плівку AgCl–Ag та у кварцове скло

*К.С.Белошенко, Л.А.Агеев, В.К.Мілославський*

У фоточутливій плівці AgCl–Ag на скляній підкладці двома симетричними лазерними пучками ( $\lambda = 532$  нм) записано голографічну ґратку (ГР) з періодом  $\Lambda = 2$  мкм. При формуванні ГР має місце нелінійний ефект самодифракції. Сформована світлом структура імплантована у кварц шляхом опромінення зразка пучком CO<sub>2</sub> лазера.